

Real-World Human-Robot Collaborative Reinforcement Learning*

Ali Shafti¹, Jonas Tjomsland¹, William Dudley¹ and A. Aldo Faisal^{1,2}

Abstract—The intuitive collaboration of humans and intelligent robots (embodied AI) in the real-world is an essential objective for many desirable applications of robotics. Whilst there is much research regarding explicit communication, we focus on how humans and robots interact implicitly, on motor adaptation level. We present a real-world setup of a human-robot collaborative maze game, designed to be non-trivial and only solvable through collaboration, by limiting the actions to rotations of two orthogonal axes, and assigning each axes to one player. This results in neither the human nor the agent being able to solve the game on their own. We use a state-of-the-art reinforcement learning algorithm for the robotic agent, and achieve results within 30 minutes of real-world play, without any type of pre-training. We then use this system to perform systematic experiments on human/agent behaviour and adaptation when co-learning a policy for the collaborative game. We present results on how co-policy learning occurs over time between the human and the robotic agent resulting in each participant’s agent serving as a representation of how they would play the game. This allows us to relate a person’s success when playing with different agents than their own, by comparing the policy of the agent with that of their own agent.

I. INTRODUCTION

Human-Machine Interaction methods are changing. Efforts were previously focused on creating “user-friendly” interfaces, so that human users can better learn to work with a system that is persistent in its behaviour. With the ever-increasing success of artificially intelligent agents, however, the possibilities for creating a fluid, adaptive and ever improving interaction are increasing. Instead of the conventional paradigm of the human adapting to the machine, we want machines that can adapt to humans – a mutual adaptation happening over time, leading to more intuitive interactions. To achieve this, we need intelligent control agents that can learn as they interact with a human user. Within Robotics, collaborative robots that learn through human interactions, are a topic of active research. A common tool for this is reinforcement learning (RL) as it follows the same learning mechanism driving human learning [1]. We are interested in implementing Human-in-the-Loop RL, i.e. having an agent that interacts and learns directly from a human counterpart.

Human in-the-loop RL can also be mapped as a specific case of a multi-agent system, which has been an ongoing area of research for the past two decades [2], [3]. However, complications arise from having a human in-the-loop, mainly due to the stochastic nature of human behaviour, and limited observability of human intent, reasoning and theory of mind.

¹ AS, JT, WD and AAF. are with the Brain and Behaviour Lab, Dept. of Bioengineering and Dept. of Computing, Imperial College London {a.shafti, a.faisal}@imperial.ac.uk

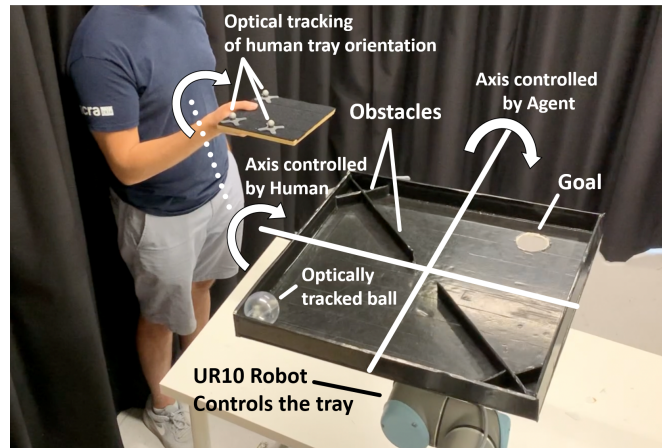


Fig. 1: Our Human-Robot co-learning setup: A ball and maze game is designed to require two players for success; one player per rotation axis of the tray. One axis is tele-operated by a human player, and the other axis by a deep reinforcement learning agent. The game can only be solved through collaboration.

Similarly, the agent is not fully observable for the human (e.g. lack of explainability), causing challenges for interactive learning.

In this paper, we present a real-world setup for studies on how humans and intelligent robotic agents can learn and adapt together for the completion of a non-trivial collaborative motor task. We have designed a human-agent collaborative maze game, see Figure 1, where a tray needs to be tilted to navigate a ball to a goal. The human controls one axis of tilt, and the agent controls the other. Hence, the agent and the human need to learn to collaborate together. We report the methods used in creating the setup, followed by experiments investigating the possibility, and results of human-robot real-time, real-world collaborative learning.

II. RELATED WORK

There is extensive literature on human-robot collaborative learning, where usually the human explicitly communicates with the agent to enhance its learning. In [4], the authors present TAMER, where the agent learns via real-time qualitative feedback from a human rather than environment reward. This is extended in [5] to work with deep RL, showing an example of human guidance in a scenario with a high dimensional state-space. This outperforms both humans and state-of-the-art RL algorithms in ATARI Bowling within 15 minutes. Sparse human feedback is investigated in [6], with less than 1% of agent actions being provided with human feedback. This method is shown to still effectively perform in ATARI and MuJoCo environments within an hour of human time. Further examples can be found in the field of shared

autonomy; environments in which multiple agents (human or artificial) act at the same time, to achieve shared or individual goals. Chen et al. [7] developed a robot which was able to exhibit socially compliant behaviour using deep RL. Reddy et al. [8] utilised deep RL, to augment a human’s actions to achieve better performance in a drone-flying task. They simulated general human models as pilots to handle the large amount of training samples required. Other works involving multi-agent systems has shown that multiple artificial agents can collaborate in complex computer games and outperform human teams [9].

Other approaches impose heuristics on agents to increase their aptitude in interacting and communicating with humans. Deep RL is used in [10] to implicitly infer social norms regarding pedestrian behaviour to improve motion planning. In [11], the agent’s speed is modulated based on how unsure of an action it is, prompting a human advisor as to when to provide feedback. In [12] human data is used to learn to predict human gaze behaviour while driving. This is then used to train better performing self-driving agents, through prediction of human visual attention. Opponent modelling and theory of mind have been leveraged to gain insights regarding RL performance in multi-agent scenarios. A learning algorithm is developed in [13] that is aware of the other learning agent, leading to better performance for both agents if playing the iterated prisoner’s dilemma with an unaware agent. In [14], meta-learning is used to learn different strategies for different species of agents, that is, agents with markedly different behaviours.

All of the aforementioned approaches are either trained in simulation, operate solely in a simulated world or are based on sequential or interval-based interactions involving explicit communication. In this work we are interested instead in real-world, real-time collaborative learning between a human and an agent, with implicit communication.

III. METHODS

A. Robotic Setup

We use a Universal Robots UR10 (Universal Robots A/S, Odense, Denmark) as the robotic manipulator. A 50cm × 50cm square tray is built out of cardboard material, and attached to the UR10 end-effector, through a 3D printed mechanical interface. The tray has barrier walls on all four sides to keep the ball from falling off as well as two obstacle walls, positioned diagonally, with a 9cm opening in the centre (refer to Figure 1 and Figure 2). A 5cm-diameter hole is cut near one of the board’s corners, representing the goal for a rolling ball to fall into. The ball is 6cm in diameter and made out of transparent acrylic. The game, i.e. the task of rolling the ball from a given start point on the tray, to the goal, is solved purely by rotating the tray around its x - y axes (two orthogonal axes on the tray plane, with the centre of the square tray as the origin – see Figure 2); no rotation around the z -axis, nor translations along any axes is allowed. The human player’s commands are sent via a smaller tray that they hold and rotate (Figure 1 and 2). The human tray’s orientation is tracked with three optical

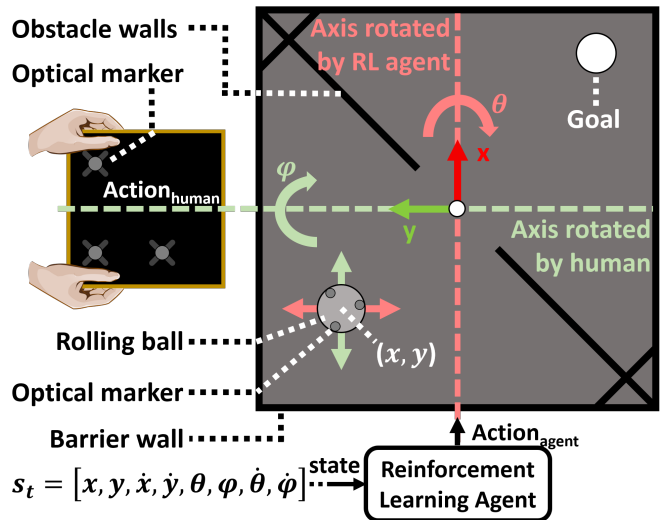


Fig. 2: Overview of our collaborative maze game setup. The human and the RL agent’s actions are mapped to orthogonal rotation axes of the tray. The individual effects of human and agent actions are marked on the ball with green and red arrows respectively. The states fed to the RL agent are x and y position of the ball in the tray frame, x and y ball velocity, rotation angles along the two axes (θ for x and ϕ for y rotations), and respective rotational velocities.

markers placed on top of it, through a motion capture system consisting of Optitrack Flex 13 cameras (NaturalPoint, Inc. DBA OptiTrack, Corvallis, Oregon, USA). The position of the ball on the tray is similarly tracked via optical markers placed inside it (Figure 1 and 2).

To integrate the above, we used the Robot Operating System (ROS) [15], running on a Linux workstation (ROS Melodic, Ubuntu 18.04). We added the tray and its attachment interface to the UR10’s Unified Robot Description Format (URDF¹) file within ROS so that its pose can be continuously tracked through ROS’s transform library (tf²). The motion capture software was running on a Windows 10 workstation transmitting the motion data through the NatNet protocol³ over the network. We used the NatNet 3 ROS driver⁴ to communicate between the motion capture system and ROS, allowing the pose of the human tray and the ball to be tracked with ROS’s transform library, and with respect to the tray frame. Human commands are then calculated with a P-control approach, the error defined as the difference of the human tray and the game tray angles, along the defined axis. To send motion commands to the robot, we used the jog_arm⁵ ROS package which simplifies the communication of smooth velocity commands to ROS-enabled robots, allowing us to send real-time jogging commands.

B. Reinforcement Learning Setup

We apply a PyTorch [16] implementation of the Soft Actor-Critic algorithm (SAC) [17], based on OpenAI’s open-

¹<http://wiki.ros.org/urdf>

²<http://wiki.ros.org/tf2>

³<https://optitrack.com/products/natnet-sdk/>

⁴https://github.com/mje-nz/natnet_ros

⁵https://github.com/UTNuclearRoboticsPublic/jog_arm

source “Spinning Up” implementation [18]. SAC is an off-policy, maximum entropy method. Running off-policy allows for the reuse of state-action transitions sampled in previous trials, which is crucial when few interaction steps are feasible. The maximum entropy framework [19] adds an entropy maximisation term to the RL reward function, encouraging exploration. This exploration/exploitation relationship can be balanced by a temperature parameter, α , where a larger α is used to encourage more exploration, and a smaller α corresponds to more exploitation. α acts as an important hyperparameter for SAC, and by using the automatic entropy tuning method introduced by Haarnoja et al. [20], the policy’s entropy can be constrained to a desired value throughout the learning process. This removes the need for intricate hyperparameter tuning, allowing for a very sample-efficient training process.

To interface the robotic setup explained in III-A, we define a eight-dimensional state space. It consists of the position and velocity of the ball along the x and y axes in the game tray frame, along with the rotation angles and rotation velocities of the game tray about its x and y axes (see Figure 2). The human behaviour is included in the state space through the game tray rotation around its y -axis, which is mimicking the human’s tray via the tele-operation interface. The RL agent’s action space is one-dimensional, a continuous value between -1 and 1 which is mapped to rotational velocity commands along the game tray’s x axis. For every time step t , the motion capture system calculates the position and orientation of both the ball and the human’s tray, while the ROS transform library gives the robot’s tray orientation. Given the observation of the current state, s_t , the policy network outputs a distribution of actions, from which an action, a_t , is sampled during training. During testing, the mean of the distribution is used, thereby removing the stochasticity, having the policy fully exploited. The action, being a velocity command, is executed on the robot for 200ms. Limits are set for both the rotational velocity, and the angles of the tray to keep the workspace safe. The resulting state s_{t+1} , reward r_t and whether or not the state was terminal, d , are then extracted and stored in a replay buffer of past transitions used to update the policy. A sparse reward function is used to penalise the agent with -1 for every time step and a reward of $+10$ if the target is reached. This means that the agent does not have explicit knowledge of the goal position, and thus experiencing goal reaches is crucial to it forming a representation of state values with respect to the goal.

C. Experimental Setup

We now have a foundation for applying human and agent actions together on the robot manipulator. Each velocity action is applied constantly for 200ms. We refer to this as a single control frame. The control frame approach, along with the loop delay, means that the human will observe a delay in their intended action being executed. We measured this to be a maximum of 300ms – actual value depending on timing of human action and how it fits with the control frame sequence. While efforts can be made to reduce this delay,

we see it as an interesting component of the system, as it adds complications to the system dynamics from the human’s point of view, making the interaction with an untrained RL agent more fair.

For our experimental setup, we define each trial to consist of 200 control frames, a total of 40 seconds. A trial ends immediately if the ball reaches the goal, and otherwise times out in 40 seconds – i.e. after 200 control frames have been applied. Each trial, therefore, consists of 200 state transitions for the RL agent, which are stored in its replay buffer, to be used for network updates. We set the size of the agent’s replay buffer to be 5 trials, meaning a buffer of 1000 (5×200) state transitions. The game always starts with the ball in one of the corners of the side of the tray opposite the goal-side, alternating between the three corners on each trial. For trial results, scores are defined on a linear scale with a maximum score of 200, and one point lost for each applied control frame – i.e. if the goal is not reached by the end of the trial, the score will be zero.

IV. EXPERIMENTS

A. Preliminary study and results

Pilot experiments of the system were conducted to evaluate its functionality and plan out for the main experiments described in the next sub-section. To closely follow the original application of SAC [21], training is counted in terms of control frames (i.e. RL agent’s state transitions), each frame followed by a single gradient update of all networks. All agent transitions are stored in the buffer without limit. Offline updates of the network based on the stored buffer are also performed to accelerate learning.

Two sets of tests were performed in this format. First, a single participant interacted with a previously untrained agent. The training process consisted of 3,500 control frames and 140,000 offline gradient updates. Offline updates were divided throughout training, running 20,000 offline updates for every 500 control frames. After completion of each of these offline updates, performance was tested in trial-based format, for 10 trials, as described before, with results reported averaged over the 10 trials, shown in Figure 3, left.

For the second sets of tests, 10 participants trained with a previously untrained agent on a trial-based manner. Participants first trained for 8 trials, with all transitions recorded in the replay buffer. The agent then undergoes 30,000 offline gradient updates on that buffer. This is followed by a second training set of 7 trials, with transitions added to the original buffer, resulting in a 15-trial long buffer. Another 30,000 offline gradient updates are applied based on the new buffer. Ten trials of testing with the agent follow, with scores averaged and reported. Each participant was then asked to do another ten trials, this time with a human “expert”, one of the system’s designers who had the most experience with the game, acting as the interaction partner for human-human trials, controlling the axis previously under control of the RL agent. During the human-human trials we ensured the two players cannot see each other, and that they do not

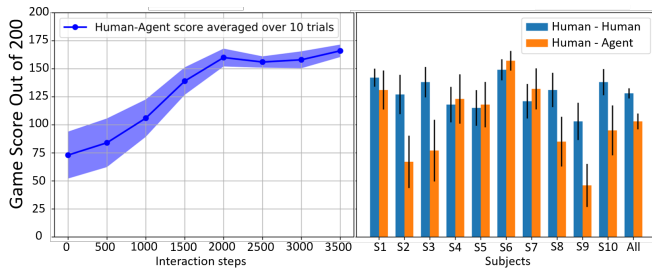


Fig. 3: Left: Learning curve of a single human player training with the agent, including both online and offline updates of the agent. Tests are performed at 500-step intervals, scores averaged over ten trials. Plot shows mean score and standard error of the mean. Right: Results of ten participants playing the game with their trained agent, and with a human expert. Mean score and standard error of the mean is shown.

communicate in any way. Score results for this are averaged over ten trials and reported in Figure 3, right.

Results from the single-subject experiment show the human-agent team as able to solve the interaction task within the time provided. Furthermore, the inconsistency of the performance is decreasing as the human-robot team learn to collaborate. This is possibly the effect of both the agent learning, and human motor adaptation. In the second experiment, the RL-agent’s ability to collaborate with humans was compared to how humans collaborate with each other. In five out of the ten preliminary participants (S1, S4, S5, S6, S7) there was no significant differences in performance between the two scenarios. The remaining half of the participants exhibit worse performance when collaborating with the agent. We observed that the players having worse results with their agents, also failed to reach the goal, or at most reached it one time, in the first 500 control frames of the game, which affects the agent’s representation of the game’s goal. This might be due to these participants being inherently worse players at the game, and would perhaps have been resolved with longer training.

B. Co-learning experiments

Having confirmed the feasibility of Human-in-the-Loop learning with our system through the preliminary study above, we move to experiments on collaborative learning. We ran 7 participants. To accelerate learning, participants start their training on a common pre-trained agent. The pre-trained agent is the result of 8 trials of interactions by the expert player from the preliminary study, followed by 30,000 offline gradient updates – total elapsed time is about 15 minutes. This is effectively half of the training done on the agents in the preliminary study. The pre-trained agent is able to navigate the ball towards the general direction of the goal, with coarse movements and low precision.

Participants are completely naive to the experimental setup. Before training starts, a description of the system is given to the participant. They are told about the RL agent, with a brief description of how RL works. They are also told about what they can control, and how to do it. Each participant is allowed to try out the interface and rotate the

tray for 40 seconds. This is without the ball on the tray, and without the RL agent acting.

Training is done in a trial-based manner, allowing us to observe performance results during training. The experience replay buffer’s length is limited to 5 trials. Training consists of 80 trials, performed in blocks of 10, with the participant given a chance to rest briefly in between blocks. The agent’s policy is not updated during the trial. At the end of each trial, the agent undergoes 200 gradient updates. No offline gradient updates are performed. Before each trial starts, the participant is alerted by three beeps played over speakers, and a trial’s end is similarly announced, by a single beep. Score results and the full state space of the agent’s data are recorded for analysis.

Once 80 trials of training are complete, the participants are tested with their own final agent, as well as four agents trained with different players. The agents are frozen during testing, and are not learning any more. Three of the four agents are selected from those of the preliminary study, namely that of S1, S5 and S7 (see Figure 3, right), which showed a performance at the same level as human-human performance. The fourth agent is the expert player’s agent, trained for 160 trials with online updates, followed by 256,000 offline gradient updates on the full buffer of 160 trials. Participants start testing by playing 10 trials with their own agent, then 10 trials each with the four other models (S1, S5, S7 and expert, randomised), and finally playing another set of 10 trials on their own agent. They are not told that their own agent is among the testing agents, but are rather told that they are being tested with 6 unspecified agents. Game score and observed data are recorded for analysis.

V. RESULTS & DISCUSSION

To interpret the results, it is important to better understand what each of the agents the participants are tested with represent. Agent S1 has an issue with one of the corners of the starting side of the tray (bottom right corner of starting side in Figure 2), causing difficulties in reaching the goal side of the tray. Once on the goal side, S1 implements movements in the correct direction, but too fast, making it difficult for a human to collaborate effectively with the agent. Agent S5 does not have issues with the starting side of the tray but, like S1, has issues with high velocity motions on the goal side. Agent S7 does not have any such issues and is therefore easier to collaborate with, although its motions are not as fine-tuned as those of the expert agent. Finally, the expert agent, having been trained on a large buffer of interactions, for a high number of iterations, implements large, yet well-controlled motions on the starting side of the tray to, with help from the human, lead the ball to the goal side. Once on the goal side, the expert agent performs very fine-tuned motions around the goal, making it easier for the human player to drop the ball into the goal, if they are capable of applying fine motions themselves.

Figure 4 shows the results of all 7 players during testing, when playing the game with all the above agents. We see a divide in the participants’ results. Looking at when

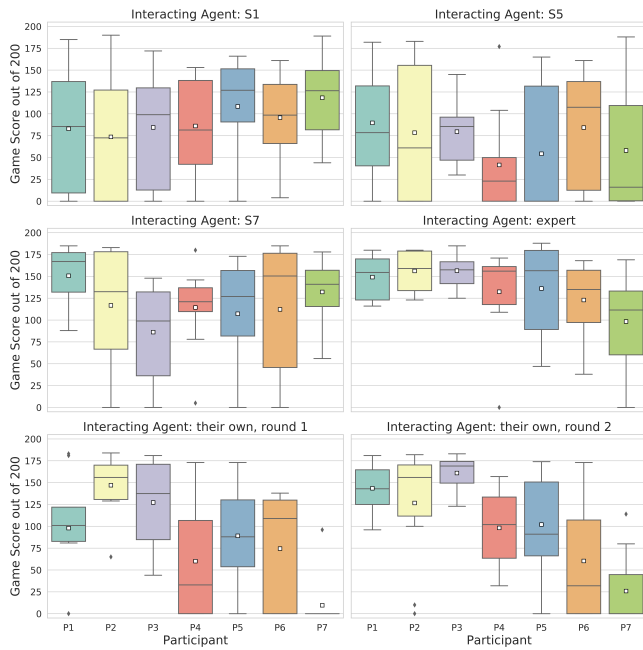


Fig. 4: Boxplots of game scores of all 7 participants (P1 to P7) playing with different agents: S1, S5, S7, expert, and their own agent twice. The white squares indicate the mean.

participants play with their own model, particularly on round 2, we see 3 participants that are performing consistently well (P1, P2, and P3). P4 and P5 have medium performances, whereas the others have bad performances (P6 and P7). This divide seems to persist with some of the other agents, e.g. when playing with the expert agent, we see that, again, P1, P2 and P3 have more consistent performance than the others. This can be explained with P5, P6, and P7 being generally bad at the game but this does not explain the results when playing with S1. In this case, P1, P2 and P3 show very inconsistent and mediocre performance, significantly lower than their performance with their own agents, whereas P5, P6 and P7 retain their average to high performance that they showed with the expert agent, and outperform their results with their own agents.

This result fits well with the hypothesis that co-learning is occurring, and that personal models are important. P1, P2 and P3 have managed to develop a consistent collaborative policy through their 80 trials, whereas this has occurred less so for P4, and even less so for P5, P6 and almost not at all for P7. However, we can already see from the results that the issue with P5, P6 and P7 is the agent they developed, and not an inherent skill issue, i.e. there exist agents that improve their game. As an example, see P7’s performance with S7, which is on level with the highest performances achieved by any participant with any agent. Perhaps this could have been achieved with their own agent with longer training, or further policy update iterations.

To further analyse this, we compare the different trained agents, independent of the human interacting with them. To do this, we “test-drive” our agents offline, by feeding them state iterations, evenly distributed to cover a fair sample of all possible state ranges for all 8 state parameters. We iterate

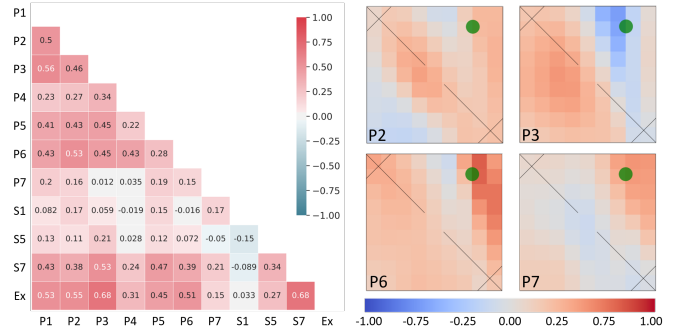


Fig. 5: Left: Correlations between the behaviour of all participant-trained agents, as well as the models they tested against, S1, S5, S7 and expert. Right: Spatial representation of trained agents’ behaviour correlation with that of the pre-model, for participants P2, P3, P6 and P7. The goal is marked as a green circle – see Figure 2 for reference. A higher correlation in a given position means that the final agent’s policy has changed less from the original pre-model on which training started.

x and y with 5.5cm intervals, \dot{x} and \dot{y} with 30cm/s intervals, tray angles along the two axes with 0.05rad intervals and respective angular velocities with 0.2rad/s intervals. Cross-iterating all the state parameters, we record output actions of the agents. This results in an output action vector of length 1,265,625 which can then be used to compare the behaviour of different agents, through correlation analysis. We look at how the participants’ policies, and the testing policies they tried out relate to each other. For this we check correlations between the different agents’ action outputs when fed the same iterations of states as inputs. The result of this can be seen in Figure 5-Left. Note that, in between the participants, the expert agent has the highest correlations with those of P1, P2 and P3 – same participants that have the best performance with it. Generally, the expert and S7 agents have the highest correlations with the participants’ agents, and they are also the agents that get the best performance from the participants, aside from their own agents - see Figure 4. S1 and S5 have the lowest correlations overall with our participants’ agents, and again this fits with the performance plots of Figure 4. The general trend observed by looking at individual participants’ agents and how they correlate with test agents, is that the higher a test agent is correlated with the participant’s own agent, the better the participant’s performance will be with it. Note that the actions of an RL agent in isolation are relating to the behaviour of the person that trained RL agent, when facing other RL agents. This is an indication that our human-in-the-loop system is leading to co-learning, creating agents that can serve as a representation of the human that trained them, in terms of their skill in this game.

In order to show the meaning of these correlations more intuitively, we present a spatial representation for 4 of the participants across the spectrum. We take P2, P3, P6 and P7. P2 and P3 show generally good performance on their own models, the expert model and S7. P6 and P7 have poor performance overall, though P7 plays well with S7. Figure 5-Right, shows how these four participants’ agents, developed their policies from the pre-model, in a spatial sense. The figure depicts the game tray, with the heatmap values re-

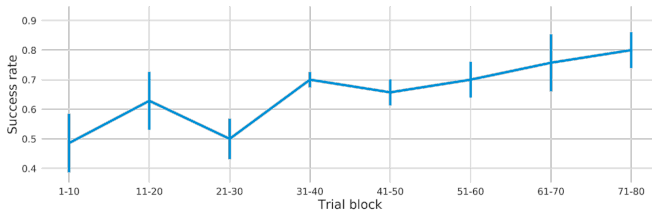


Fig. 6: Success rate (reaching the goal) for all 7 participants as they went through 80 trials of training, in 10-trial blocks, serving as the learning curve. Mean and standard error of the mean across all participants shown.

flecting the correlation of the participant’s agent’s behaviour in each position, with that of the pre-model on which they started the training. A high correlation means that the pre-model’s policy has been retained, whereas lower correlations correspond to higher degrees of change in policy. The pre-model has a good policy around the barrier, and is capable of helping participants get to the goal side of the game. On the goal side however, and particularly the corner closest to the goal, it does not have the best policy: it implements very coarse actions that are hard to coordinate with. We see these reflected in the four participants’ policy changes: P2 and P3 have made bigger changes to the policy near the goal, and smaller changes around the barrier, whereas P6 and P7 have done the reverse. This is reflected in their performance results.

Finally, figure 6 is learning curve based on success rate, i.e. number of times reaching the goal, within 10-trial blocks. Mean values and standard error of the mean across all 7 participants are shown. We see the beginning of a plateau occurring towards the end of the training phase.

VI. CONCLUSIONS

We presented a real-world, human-in-the-loop, reinforcement learning setup for studies on human-robot collaborative learning. The setup consists of a non-trivial ball and maze game, which can only be solved through effective collaboration. We initially tested out the system on pilot experiments, to confirm feasibility of real-world learning with the setup. Tested with 1 subject over a long period of iterations we see constant improvement and a plateau in the learning curve. Tested with 10 participants for a shorter period, we see that half of the participants reach human-human collaborative performance levels.

Based on the above outcomes, we designed experiments for investigation into human-robot co-learning. We tested 7 participants, for 80 trials, training with an RL agent with minimal pre-training. Our results show that with a human in-the-loop it is possible to settle on an effective collaborative policy that leads to consistent success in the game. This is, however, variable across participants, and highly dependent on the particular participant’s behaviour during training with the RL agent. We see this confirmed through analysis on how agents of different participants correlate across, and with the test agents. Effectively, we are able to relate a human player’s performance with new agents that are not their own, by looking at how similar the new agents’ policy is to that of

their own agent. We intend to continue experimenting with this setup to further explore the intricacies of human-robot collaborative learning and motor adaptation.

REFERENCES

- [1] D. M. Wolpert, J. Diedrichsen, and J. R. Flanagan, “Principles of sensorimotor learning,” *Nature Reviews Neuroscience*, vol. 12, no. 12, pp. 739–751, 2011.
- [2] P. Stone and M. Veloso, “Multiagent Systems : A Survey from a Machine Learning Perspective 1 Introduction 2 Multiagent Systems,” *Autonomous Robots*, vol. 8, no. 3, p. 345–383, 1997.
- [3] P. Hernandez-Leal, B. Kartal, and M. E. Taylor, *A survey and critique of multiagent deep reinforcement learning*, vol. 33. Springer US, 2019.
- [4] W. B. Knox and P. Stone, “Interactively shaping agents via human reinforcement: The TAMER framework,” *K-CAP’09 - Proceedings of the 5th International Conference on Knowledge Capture*, pp. 9–16, 2009.
- [5] G. Warnell, N. Waytowich, V. Lawhern, and P. Stone, “Deep TAMER: Interactive agent shaping in high-dimensional state spaces,” *32nd AAAI Conference on Artificial Intelligence, AAAI 2018*, pp. 1545–1553, 2018.
- [6] P. F. Christiano, J. Leike, T. B. Brown, M. Martic, S. Legg, and D. Amodei, “Deep reinforcement learning from human preferences,” *Advances in Neural Information Processing Systems*, vol. 2017-Decem, no. Nips, pp. 4300–4308, 2017.
- [7] Y. F. Chen, M. Everett, M. Liu, and J. P. How, “Socially aware motion planning with deep reinforcement learning,” in *2017 IEEE/RSJ International Conference on Intelligent Robots and Systems (IROS)*, pp. 1343–1350, IEEE, 2017.
- [8] S. Reddy, A. D. Dragan, and S. Levine, “Shared autonomy via deep reinforcement learning,” in *Robotics: Science and Systems (RSS) 2018 conference*, 2018.
- [9] C. Berner, G. Brockman, B. Chan, V. Cheung, P. Dębiak, C. Dennison, D. Farhi, Q. Fischer, S. Hashme, C. Hesse, *et al.*, “Dota 2 with large scale deep reinforcement learning,” *arXiv preprint arXiv:1912.06680*, 2019.
- [10] Y. F. Chen, M. Everett, M. Liu, and J. P. How, “Socially aware motion planning with deep reinforcement learning,” *IEEE International Conference on Intelligent Robots and Systems*, vol. 2017-Sept, pp. 1343–1350, 2017.
- [11] J. Macglashan, R. Loftin, M. L. Littman, D. L. Roberts, and M. E. Taylor, “A Need for Speed : Adapting Agent Action Speed to Improve Task Learning from Non-Expert Humans Categories and Subject Descriptors,” *Aamas 2016*, pp. 957–965, 2016.
- [12] A. Makrigiorgos, A. Shafti, A. Harston, J. Gerard, and A. A. Faisal, “Human visual attention prediction boosts learning & performance of autonomous driving agents,” *arXiv preprint arXiv:1909.05003*, 2019.
- [13] J. Foerster, R. Y. Chen, and P. Abbeel, “Learning with Opponent-Learning Awareness,” pp. 122–130, 2018.
- [14] N. C. Rabinowitz, F. Perbet, H. F. Song, C. Zhang, and M. Botvinick, “Machine Theory of mind,” *35th International Conference on Machine Learning, ICML 2018*, vol. 10, pp. 6723–6738, 2018.
- [15] M. Quigley, K. Conley, B. Gerkey, J. Faust, T. Foote, J. Leibs, R. Wheeler, and A. Y. Ng, “Ros: an open-source robot operating system,” in *ICRA workshop on open source software*, vol. 3, p. 5, Kobe, Japan, 2009.
- [16] A. Paszke, S. Gross, F. Massa, A. Lerer, J. Bradbury, G. Chanan, T. Killeen, Z. Lin, N. Gimelshein, L. Antiga, *et al.*, “Pytorch: An imperative style, high-performance deep learning library,” in *Advances in Neural Information Processing Systems*, pp. 8024–8035, 2019.
- [17] T. Haarnoja, A. Zhou, P. Abbeel, and S. Levine, “Soft actor-critic: Off-policy maximum entropy deep reinforcement learning with a stochastic actor,” in *Proceedings of the 35th International Conference on Machine Learning*, 2018.
- [18] J. Achiam, “Spinning Up in Deep Reinforcement Learning,” 2018.
- [19] B. D. Ziebart, A. Maas, J. A. Bagnell, and A. K. Dey, “Maximum entropy inverse reinforcement learning,” in *Proceedings of the Twenty-Third AAAI Conference on Artificial Intelligence*, 2008.
- [20] T. Haarnoja, A. Zhou, S. Ha, J. Tan, G. Tucker, and S. Levine, “Learning to walk via deep reinforcement learning,” in *Robotics: Science and Systems (RSS) 2019 conference*, 2019.
- [21] T. Haarnoja, A. Zhou, K. Hartikainen, G. Tucker, S. Ha, J. Tan, V. Kumar, H. Zhu, A. Gupta, P. Abbeel, *et al.*, “Soft actor-critic algorithms and applications,” *arXiv preprint arXiv:1812.05905*, 2018.